ARID ZONE JOURNAL OF ENGINEERING, TECHNOLOGY & ENVIRONMENT
AZOJETE March 2025. Vol.21(1):145-156
Published by the Faculty of Engineering, University of Maiduguri, Maiduguri, Nigeria.
Print ISSN: 1596-2490, Electronic ISSN: 2545-5818
www.azojete.com.ng

ORIGINAL RESEARCH ARTICLE

IMPLEMENTATION OF THYRISTOR BASED CONTROL OF SEPARATELY EXCITED DC MOTOR DRIVEN BY SINGLE-PHASE SEMI-CONVERTER

G. C. Diyoke[1*], C. A. Okeke[1] and C. Ezugwu[2]

[1]*Department of Electrical and Electronic Engineering, Michael Okpara University of Agriculture, Umudike, Abia State, Nigeria.*

[2]*Department of Electrical and Electronic Engineering Technology, Federal Polytechnic, Nasarawa, Nasarawa State, Nigeria.*

[*]*Corresponding author's email address: geraldiyoke@mouau.edu.ng*

ARTICLE INFORMATION

Submitted: 5th September 2024
Revised: 24th December 2024
Accepted: 3rd February 2025

Keywords:
Semi-converter
Dc motor
Armature voltage
Field current
Speed
Torque

ABSTRACT

This paper presents the implementation of thyristor-based control for a separately excited DC motor using a single-phase semi-converter. The study focuses on the design, operation, and performance analysis of the system, highlighting its ability to efficiently control the motor's speed and torque. The semi-converter, consisting of thyristors, provides variable DC voltage to the motor by controlling the firing angle, enabling precise regulation of motor parameters. Key aspects, such as circuit design, firing angle control, and power quality considerations, are discussed in detail. Computer aided simulation results demonstrate the effectiveness of the proposed system in achieving smooth and reliable motor control with improved energy efficiency. The findings underline the applicability of thyristor-based control in industrial and automation applications, offering a cost-effective solution for DC motor drives. It is observed that the method of voltage control shows that a rated voltage of 200 V, the rated speed of 1500 RPM and torque of 10.5 N-m cannot be exceeded. The method of field flux control shows that a rated voltage, the rated speed can be exceeded to reach 208 V and 3000 RPM respectively while the rated torque cannot be reached.

1.0 Introduction

In order to control the dc motor speed (Poomima et al., 2006), the thyristor semi-converter provides a variable output voltage. A direct current (DC) motor is a machine that converts DC electrical energy into rotating mechanical energy and are rated in horsepower (Onah et al., 2022 and Asadi et al., 2019). Due to the simplicity, high power conversion efficiency, low cost of operation of the system, reliability, controllability (Perelmuter 2012; Nguyen et al., 2019; Rashag 2019; Sami et al., 2021 and Duby et al., 2022) and maintainability, it is widely used in industrial and domestic applications as reported by kandpal et al., (2015); Hareb et al., (2021); Virendra et al., (2013) and Sharma et al., (2016). Some of the applications are in dc drive systems for paper production, photographic film manufacturing, machine tools, traction, crude oil pipelines, variable-speed drives for woodworking machines, rolling mills, and traction drives as presented by El-Kholy et al., (2004) and Tiwari et al., (2019), adjustable-speed drive systems for textiles, renewable energy systems for wind turbine, solar tracking, home applications for vacuum cleaner, washing machines, electric razors, blender, food processor. Another vital merit of the system is that it requires no extra circuitry for commutation process (Hughes 2006 and Krishnan 2001). Separately excited dc motors are often used in applications needing precise control of speed and torque over a wide range (Hassan et al., 2023; and Hameed and Ali 2016). The report by Amed et al. (2023) detailed the study of microcomputer-based torque control of dc separately excited motor using the proportional integral (PI) controller. Based on the performance indices, semi-converter performs better than full-converter systems.

A rectifier is a type of power electronics converter that performs a conversion of electrical energy from one form to another (Namdeo et al., 2014). Semi-converter uses both thyristors and diodes for power conversion. It is simple to control, economical based on cost and more reliable during the operation. It operates by controlling the conduction angle of the thyristors, which regulates the amount of power transferred. The armature current in general is non-continuous at high values of the firing angle, high motor speed and low values of machine torque. An external armature circuit choke can be applied to promote continuous armature current operation. Rectifiers play a vital role in various industrial, commercial and renewable energy applications, offering flexibility and efficiency in power conversion processes. Some of its applications are as follows: motor drives, dc power supply, heating systems, renewable energy, HVDC transmission, battery charging systems, etc. Speed control in a DC separated excited motor can be achieved through various methods, each offering different advantages and suitability depending on the application requirements. Here are some common methods of speed control for DC separated excited motors: (1) armature voltage control: this achieved by varying the voltage applied (Duby 2009 and Saini et al., 2020) to the armature winding of the motor, thereby the motor speed can be controlled; (2) field flux control: this is realized by adjusting the field winding excitation, the magnetic flux within the motor can be varied, affecting its speed-torque characteristics.

2. Materials and Method

2.1 Single-phase Semi-Converter Configuration and Operation

In Figure 1, a semi-converter circuit configuration fed with separately excited dc motor is developed. The power circuit consists of two controlled power thyristors T_1 and T_4, two power diodes D_2 and D_3, and one freewheeling diode D_F. The ac source V_s is given by $V_m sin\omega t$, where V_m is the amplitude and ω is the source frequency in rad/sec. The two similar power circuit are responsible for armature voltage and current and field voltage and current respectively. The load is modeled as series combination of a dc motor with R_a and L_a as armature resistance and inductance and E as the induced emf applied for variable-speed motor drives.

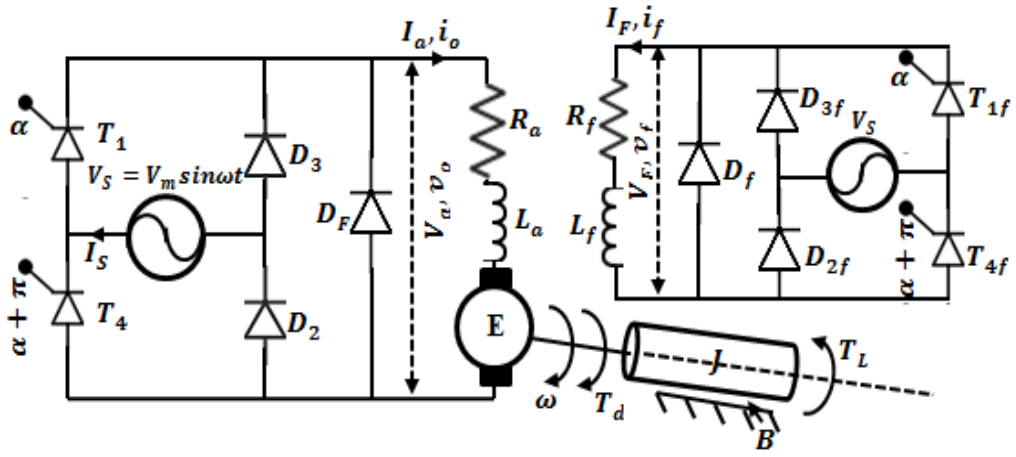

Figure 1: Semi-converter-fed separately excited dc motor configuration

Corresponding author's email address: geraldiyoke@mouau.edu.ng

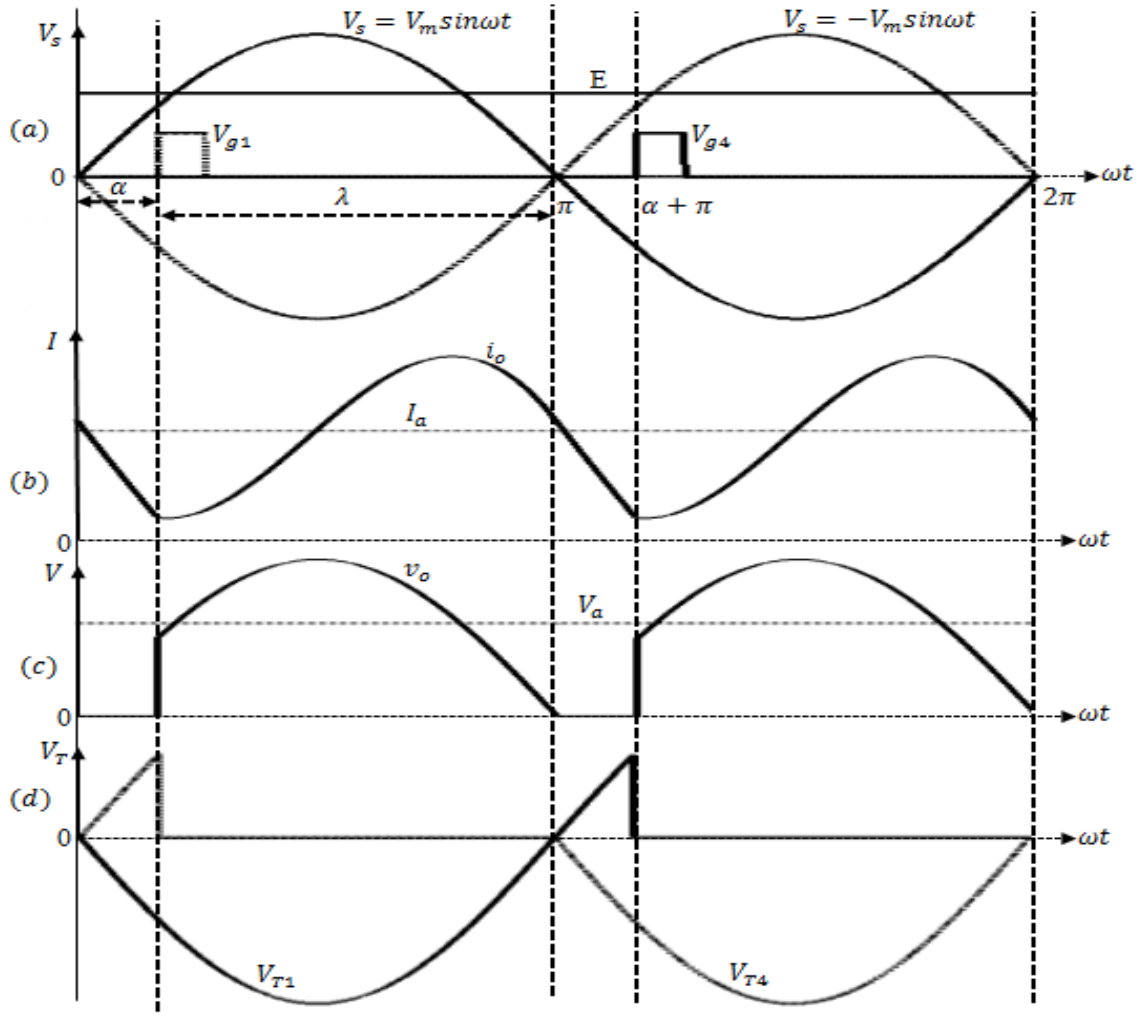

Figure 2: Waveforms of Semi-converter mode of operation.

Operation of the semi-converter circuit depicted in Figure 2; and Figure 2(a) depicts the supply voltage, dc motor EMF and gate pulses plots against the ωt (Radians). The output and armature currents are shown in Figure 2(b), under continuous current mode of operation. Waveforms shown in Figure 2(c and d) are analyzed as follows:

At interval $\alpha \leq \omega t \leq \pi$, the gate signal i_{g1} is high, T_1 and D_2 conduct current in this interval. That is, output voltage $V_o = V_m sin\omega t$; voltage drop across thyristor T_4, $V_{T4} = 0$; and voltage drop across thyristor T_1, $V_{T1} = -V_m sin\omega t$; This operation puts the thyristor and diode (T_4 and D_3) into a reverse biased mode. Also, at the interval $\alpha+\pi \leq \omega t > 2\pi$, the gate signals i_{g4} is high, T_4 and D_3 conduct current during this operation. In both intervals the output current $i_o > 0$. For, $V_o = V_m sin\omega t$; and $V_4 = -V_m sin\omega t$; D_3 conducting current. However, the system performance can be further obtained through the Fourier analysis and some notations used in this work are V_a is armature voltage, I_a is armature current, R_a is armature resistance, L_a is armature inductance, V_m is peak voltage, T_F is field torque, T_d is developed torque, P_F is the field power, P_d is the developed torque, I_F is the field current, α is the firing angle for armature voltage, α_F is the field circuit firing angle.

In Fourier series, the output voltage $v_o(\omega t)$ as depicted in Figure 2(c) for continuous current operation is expressed as:

$$v_o(\omega t) = V_a + \sum_{n=1}^{\infty} (V_{an} cosn\omega t + V_{bn} sinn\omega t) \quad 1$$

Referring to Figure 2(c), we can derive the formular for computing the armature load voltage V_a

Corresponding author's email address: geraldiyoke@mouau.edu.ng

$$V_a = \frac{1}{\pi}\left[\int_{\alpha}^{\pi} v_o d(\omega t)\right] = \frac{V_m}{\pi}(cos\alpha + 1) \quad 2$$

The rectifier output voltage as a function of ωt is given by

$$v_o(\omega t) = \frac{V_m}{\pi}\left\{(cos\alpha + 1) + \sum_{n=2,4,6,..}^{\infty}\left(\left[\frac{cos\alpha(n+1)+1}{(n+1)} - \frac{cos\alpha(n-1)+1}{(n-1)}\right]cosn\omega t + \left[\frac{sin\alpha(n+1)}{(n+1)} - \frac{sin\alpha(n-1)}{(n-1)}\right]sinn\omega t\right)\right\} \quad 3$$

The nth harmonic amplitude C_n is given as in equation (5)

$$C_n = V_n = \sqrt{V_{an}^2 + V_{bn}^2} \quad 4$$

$$V_n = \frac{2V_m}{\pi(n^2-1)}[cos^2\alpha - n^2cos^2\alpha + 2\cos(n\alpha)\,cos\alpha + n^2 + 2n\sin(n\alpha)\,sin\alpha + 1]^{\frac{1}{2}} \quad (5)$$

While the phase magnitude is developed as

$$\emptyset_n = \tan^{-1}\left(\frac{b_n}{a_n}\right) \quad 6$$

$$\emptyset_n = \tan^{-1}\left(\frac{n-1\big(sin\alpha(n+1)\big) - n + 1(sin\alpha(n-1))}{n-1(cos\alpha(n+1)+1) - n + 1(cos\alpha(n-1)+1)}\right) \quad 7$$

Where, $Z_n = \sqrt{R_a^2 + (n\omega L_a)^2}$ and $\theta_n = \tan^{-1}\left(\frac{n\omega L_a}{R_a}\right)$

The root mean square voltage can be computed by equation (8)

$$V_{orms} = \frac{1}{\pi}\left[\int_{\alpha}^{\pi} v_o^2 d(\omega t)\right] = \frac{V_m}{\sqrt{2\pi}}\left[\pi - \alpha + \frac{sin2\alpha}{2}\right]^{\frac{1}{2}} \quad 8$$

The average load or armature current I_a then becomes:

$$I_a = \frac{V_a - E}{R_a} \quad 9$$

In Fourier series, the output current $i_o(\omega t)$ as depicted in Figure 2(b) for continuous current operation is expressed as:

$$i_o(\omega t) = \frac{\frac{V_m}{\pi}(cos\alpha + 1) - E}{R_a} + \sum_{n=2,4,6,..}^{\infty}\frac{1}{Z_n}(V_{an}\cos(n\omega t - \theta_n) + V_{bn}\sin(n\omega t - \theta_n)) \quad 10$$

The rms load current, I_{arms} is calculated using

$$I_{arms} = \sqrt{I_a^2 + \sum_{n=2,4,6...}^{\infty} I_{rn}^2} \quad 11$$

Corresponding author's email address: geraldiyoke@mouau.edu.ng

Where, the n^{th} rms ripple load current I_{rn} is given as

$$|I_{rn}| = \frac{V_n/\sqrt{2}}{\sqrt{R_a^2 + (n\omega L_a)^2}} \quad 12$$

The power delivered to the dc motor is computed using

$$P_d = I_{arms}^2 R_a + I_a E \quad 13$$

The supply power factor can be computed using the formula

$$pf = \frac{I_{arms}^2 R_a + I_a E}{V_s I_{arms}} \quad 14$$

The form factor for separately excited dc motor armature current is defined as

$$Form\ factor, FF = \frac{I_{arms}}{I_a} = \frac{R_a I_{arms}}{\frac{V_m}{\pi}(cos\alpha + 1) - E} \quad 15$$

2.2 Separately excited dc motor operation and analysis

In separately excited dc motor, the field and armature voltages can be controlled independent of each other. Therefore, when the electric field current (I_F) flows in the field winding of the machine, then magnetic field is created which exerts a magnetic force on the rotor or armature coils carrying the current (I_a), causing the rotor to rotate. During this process a back EMF (E) is induced in the armature winding as it rotates.

The basic equations of the dc motor for steady-state operation can be generated as follows [1]:

$$V_a = E + I_a R_a \ = K\omega_m + I_a R_a \quad 16$$

Generated EMF, speed, flux and number of conductors in the armature is related as:

$$E = \frac{pZ}{c}\phi\left(\frac{2\pi N}{60}\right) = k\phi\omega_m = kI_F\omega_m = K\omega_m \quad 17$$

The field current $I_F$is directly proportional to the flux, ϕ. Where p implies number of poles, N is motor speed in RPM, ϕ is useful flux per pole entering or leaving the armature in weber, k is machine constant, Z is total number of armature conductors, c is number of parallel paths through winding between positive and negative brushes and ω_m is the motor speed in rad/sec.

Multiplying equation (16) by armature current (I_a) gives the total electrical power delivered to the armature P_E, loss due to armature resistance P_L in the circuit and Mechanical power developed by the armature P_M as depicted in equation (18)

$$V_a I_a(P_E) = EI_a(P_M) + I_a^2 R_a(P_L) \quad 18$$

From Equation (18), the torque developed by the armature T_d is given by

$$T_d = KI_a \quad 19$$

where, $EI_a = k\phi\omega_m I_a = T_d\omega_m$

Each thyristor blocking voltage is depicted in Figure 1(d), this plot aids in selection of the thyristor current and voltage values.

Corresponding author's email address: geraldiyoke@mouau.edu.ng

2.3 Armature and Field Voltages, Currents, firing angles, Speeds and Torque relationships

Armature control of a separately excited dc motor involves adjusting the supply voltage to the armature winding of the motor to control its speed and torque. To regulate motor's speed and torque, field control involves adjusting the field winding's current. By varying the field current, the motor's flux can be controlled, which will affect speed, torque and efficiency performance. Under steady-state conditions, armature voltage is related with firing angle as derived Equation (2). From Equation (16), the motor speed yields

$$\omega_m = \frac{1}{K}\left(\frac{V_m}{\pi}(cos\alpha + 1) - I_a R_a\right) = \frac{V_m}{\pi K}(cos\alpha + 1) - \frac{T_d}{K^2}R_a \quad 20$$

Equation (20) depicts speed relationship with developed torque. Developed motor torque can be deduced from eqn. (20) as:

$$T_d = \frac{K^2}{R_a}\left(\frac{V_m}{\pi}(cos\alpha + 1) - \omega_m\right) \quad 21$$

And developed motor power is depicted in equation (22) as

$$P_d = T_d\omega_m \quad 22$$

From Figure (1), since both armature voltage and field winding voltage are supplied by the same power circuit topology, therefore, the field circuit V_F can be obtained as

$$V_F = \frac{V_m}{\pi}(\cos(\alpha_F) + 1) \quad 23$$

The field current I_F is given as

$$I_F = \frac{V_F}{R_f} = \frac{V_m}{\pi R_f}(cos\alpha_F + 1) \quad 24$$

Based on Equations (16) and (17), the relationship between the armature and field currents is given as:

$$I_a = \frac{1}{R_a}\left(\frac{V_m}{\pi}(cos\alpha + 1) - kI_F\omega_m\right) \quad 25$$

From Equations (19), (24) and (25), the motor torque developed can be expressed as

$$T_F = kI_F I_a = \frac{kV_m}{\pi R_f R_a}\left((cos\alpha_F + 1)\left(\frac{V_m}{\pi}(cos\alpha + 1) - kI_F\omega_m\right)\right) \quad 26$$

$$P_F = T_F\omega_m \quad 27$$

3. Results and Discussion

3.1 Semi-converter

The output voltages and currents of a semi-converter depend on several factors including the topology of the converter circuit, the type of power switch devices used, the control strategy employed, and the load connected to the converter. The output voltage $v_o(\omega t)$ of Equation 3 is typically a pulsating DC waveform as depicted in Figure 2. The resulting voltage waveform varies between 0 V and 325 V. The average output voltage of a rectifier circuit can be calculated using Equation 2 and also called the armature voltage, V_a. The output current $i_o(\omega t)$ of Equation 10 is typically also a pulsating DC waveform as depicted in Figure 3 and the resulting current waveform varies between 4 A to 28 A. Equation 9 shows the formular for the average output current otherwise called armature current, I_a. The harmonics in the output voltage waveform versus firing angle is depicted in Figure 4. The highest normalized harmonic amplitude occurred at n equal to 2 with 60 degrees firing angle.

Corresponding author's email address: geraldiyoke@mouau.edu.ng

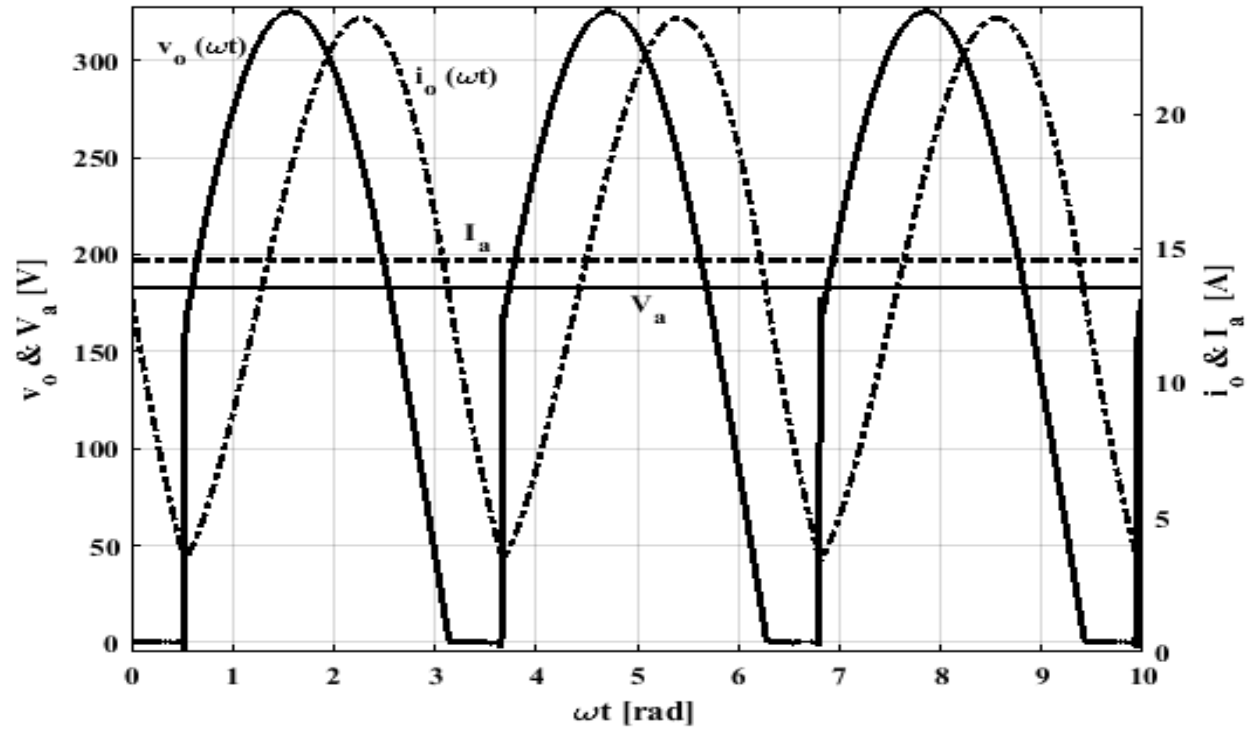

Figure 3: Outputs voltages and currents waveforms

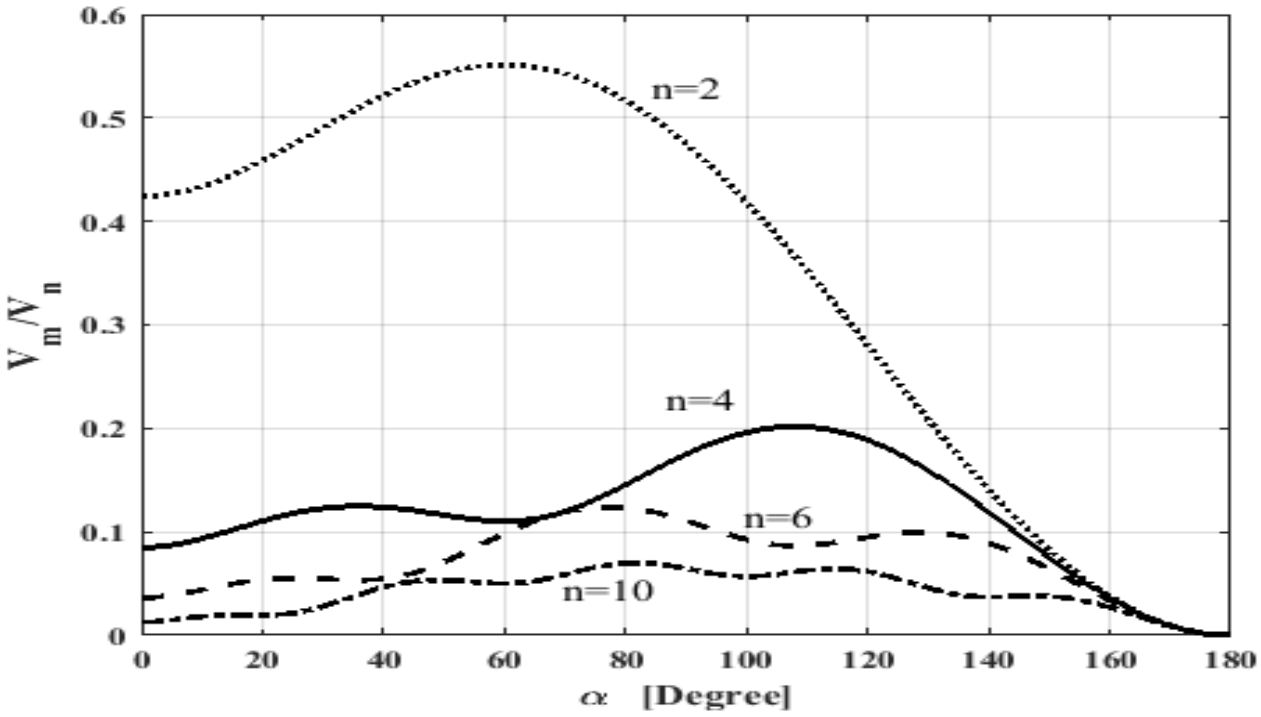

Figure 4: Harmonic index against firing angle plot

3.2 Separately excited dc motor

The relationship between armature and field voltages and currents against developed torque in a separately excited DC motor is depicted in Figure 5. However, generally, increasing the armature voltage increases the torque output of the motor, up to a point of diminishing returns and saturation effects. The speed is directly influenced by the armature voltage and current as depicted in Figure 6. Also, the speed is inversely influenced by the field voltage and current. Armature and field voltages and currents are plotted against the firing angles as shown in Figure 7. It is observed that the increase in firing angle indirectly affects the armature and field

Corresponding author's email address: geraldiyoke@mouau.edu.ng

voltages and currents. The relationship between the machine speed, current and torque is depicted in Figure 8. The armature and field powers and torques in a separately excited DC motor are influenced by the armature voltage, armature current, field voltage, field current, and mechanical load as depicted in Figure 9. The machine speed is determined by the balance between the mechanical output torque, load torque, and the motor's characteristics. Adjusting the armature voltage and field current can control the motor's speed and torque characteristics, allowing for precise speed regulation and torque control in various applications. The three-dimensional waveform of torque, power and machine speed is as plotted in Figure 10.

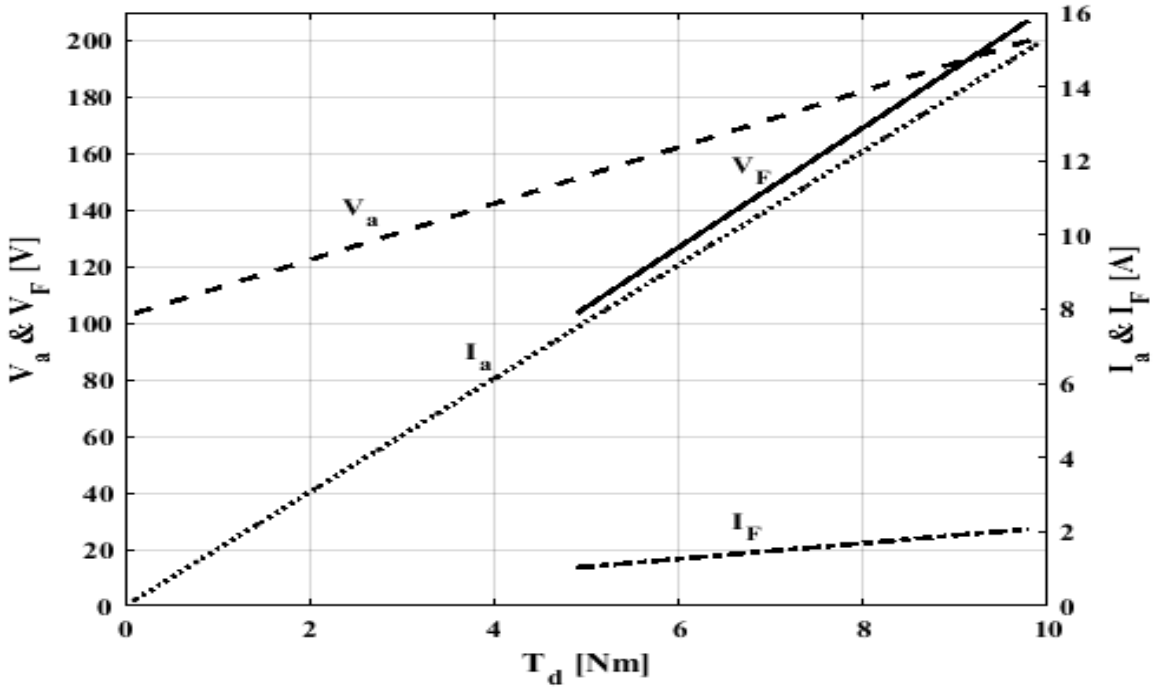

Figure 5: Armature and field voltages and currents against torque

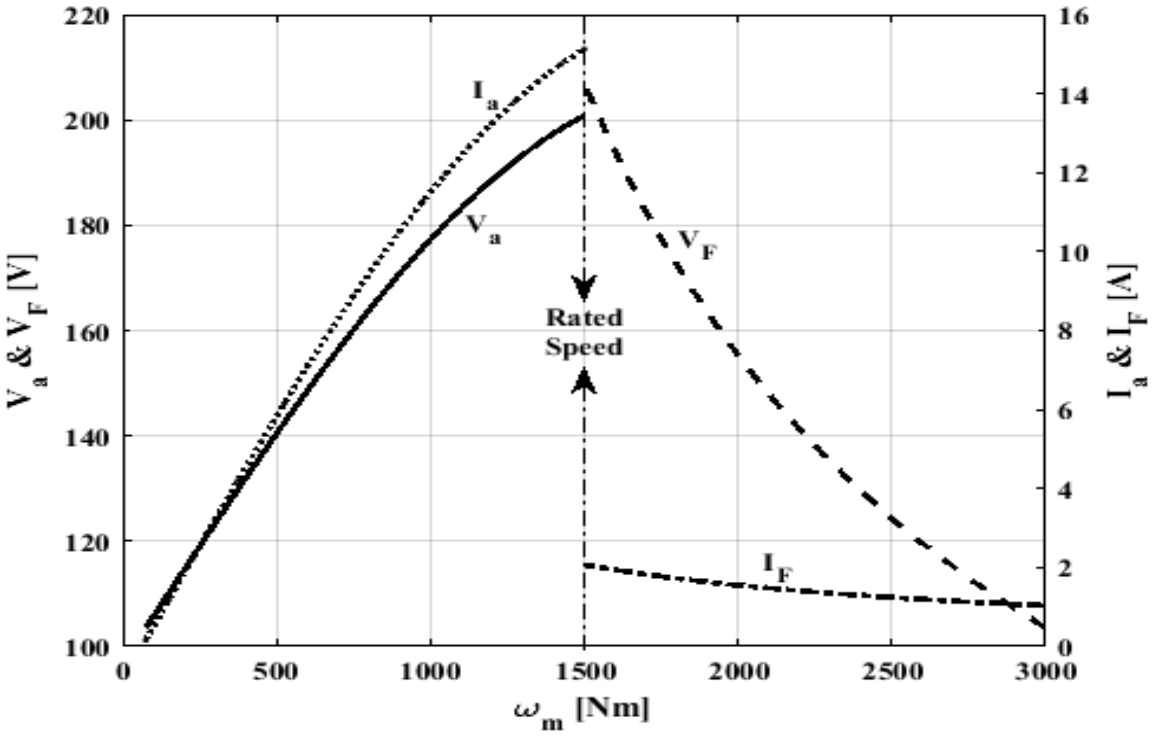

Figure 6: Armature and field voltages and currents against machine speed

Corresponding author's email address: geraldiyoke@mouau.edu.ng

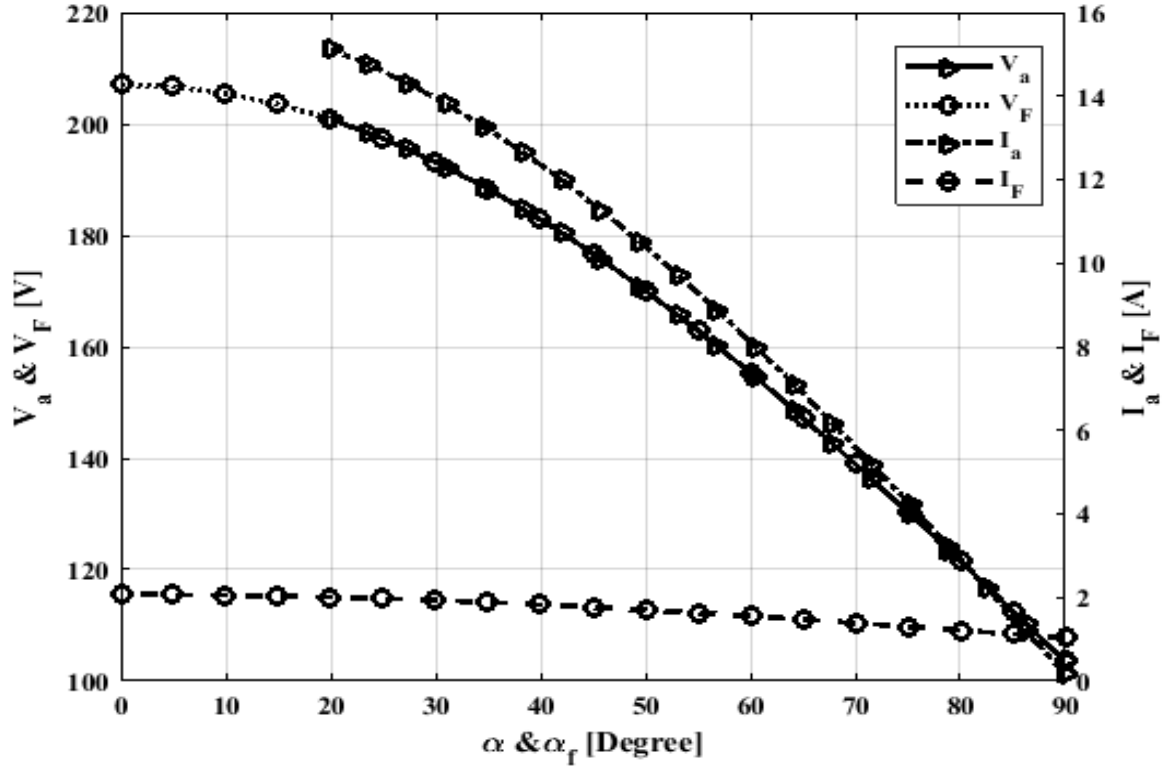

Figure 7: Armature and field voltages and currents against firing angles

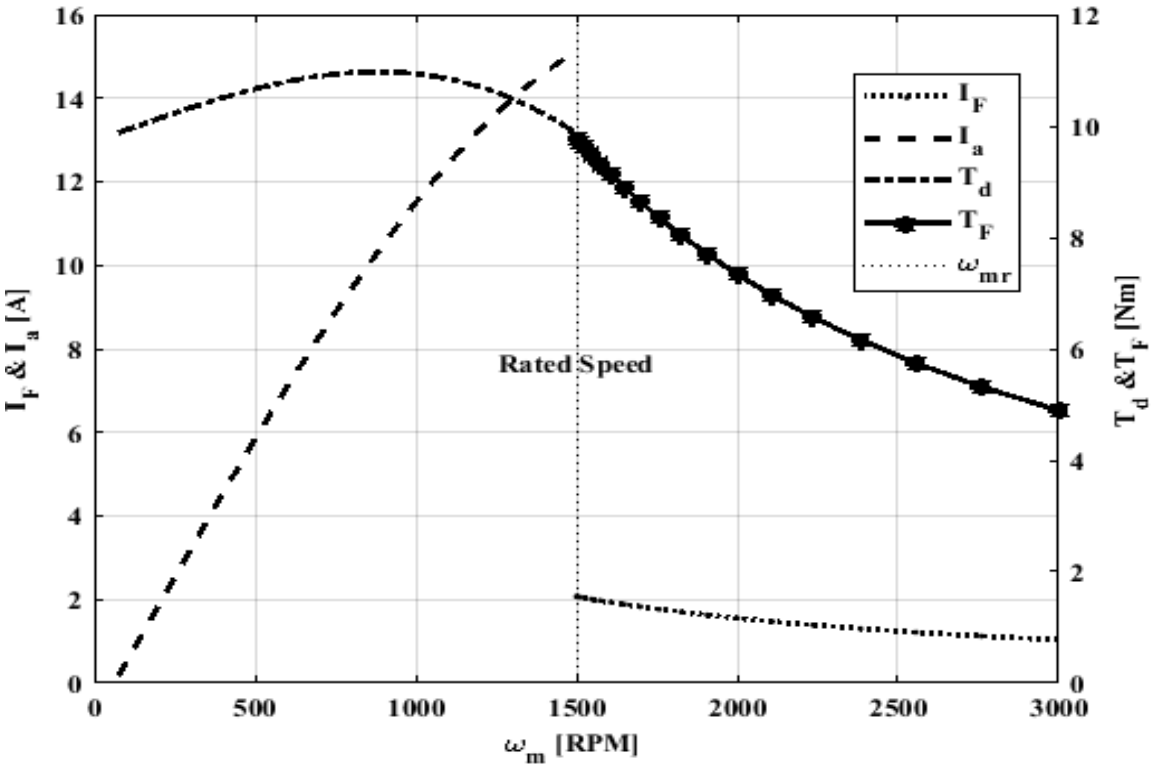

Figure 8: Armature and field currents and torques against machine speed

Corresponding author's email address: geraldiyoke@mouau.edu.ng

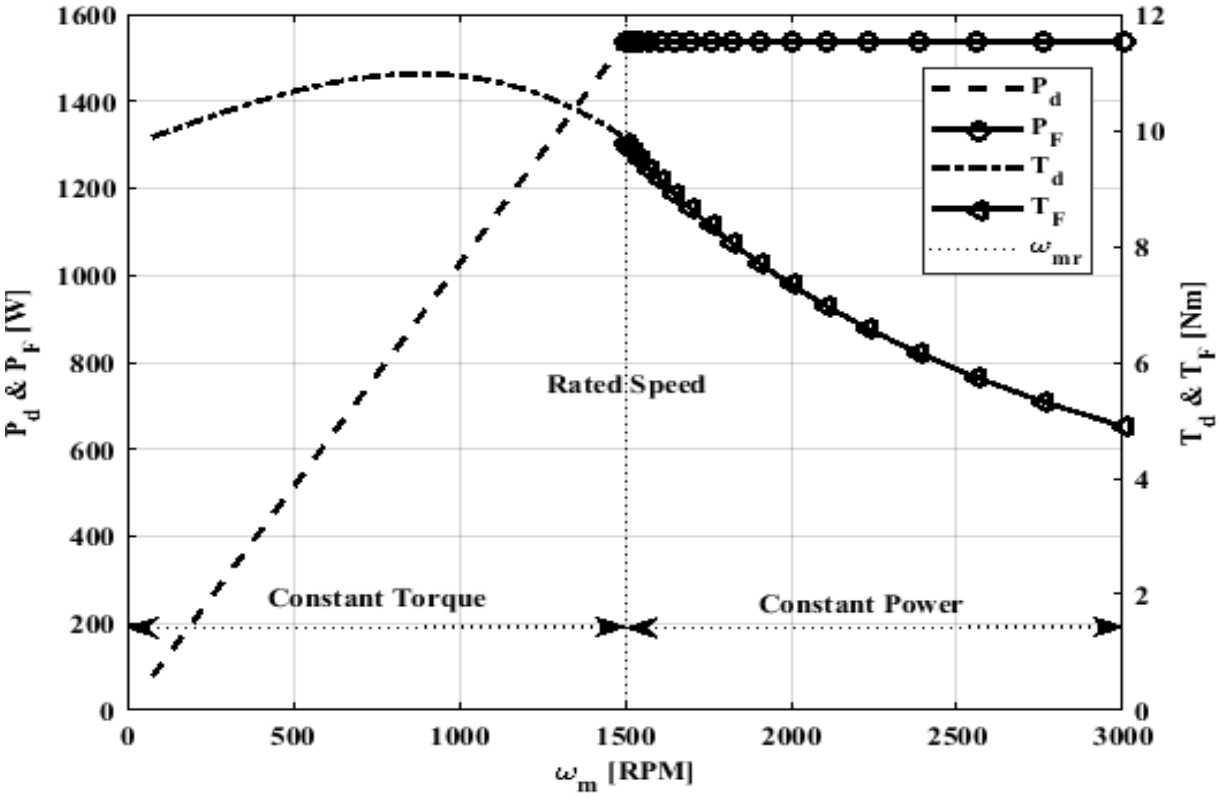

Figure 9: Armature and field powers and torques against machine speed

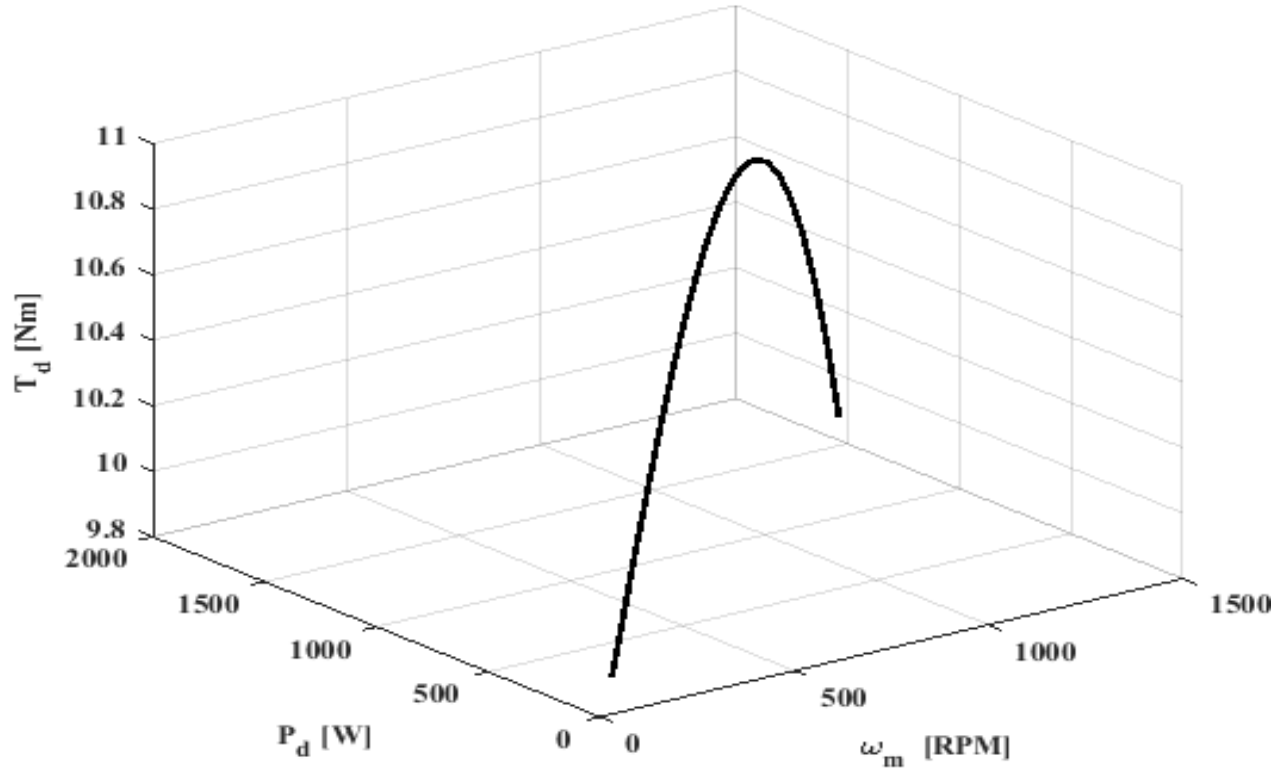

Figure 10: Three-dimensional waveform of torque, power and machine speed

Corresponding author's email address: geraldiyoke@mouau.edu.ng

Table 1: Parameters for separately excited dc motor drive

Parameter	Value
V_s	$230\sqrt{2}\sin\omega t$ V
Motor EMF, E	200 V
R_a	6.5 Ω
L_a	25mH
I_a	15 A
$\alpha = \alpha_f$	15^o
F	50 Hz
N	1500 RPM
R_f	120

4. Conclusion

The implementation of thyristor-based control for a separately excited DC motor driven by a single-phase semi-converter demonstrates significant advancements in the precise control of motor speed and torque. The system leverages the ability of thyristors to modulate voltage and current supplied to the motor, enabling effective control over its operational parameters.

This approach offers several advantages, including improved efficiency, reduced energy consumption, and enhanced system reliability. By providing smooth and adjustable control, the method ensures optimal performance across a wide range of load conditions, making it particularly suitable for industrial and automation applications. Moreover, the use of a single-phase semi-converter simplifies the design and reduces the overall cost, without compromising the system's control accuracy. This implementation highlights the potential for further integration of power electronics and motor control technologies to achieve more compact, efficient, and versatile systems.

Future work could explore extending this control strategy to multi-phase converters, incorporating advanced control algorithms, and addressing harmonics to further improve performance and reduce electrical noise.

References

Ahmed, MMR., Elemary, AA., Alaas, ZM. and Hamada, AM. 2023. Torque Control of a 5 kW, 220 V Separately excited DC Motor using Microcomputer, International Journal of Power Electronics and Drive Systems (IJPEDS), 14(2): 727 – 740.

Asadi, F. and Eguchi, K. 2019. Comparison of Different DC Motor Modeling Techniques, Journal of Electronic Research and Application, 2(2): 1 – 4.

Dubey, GK. 2009. Fundamentals of Electrical Drives, Narosa Publishing House, New Delhi Chennai Mumbai Kolkata, 60 - 139.

Dubey, T. and Sharma, JK. 2022. Efficient Speed Control of Thyristor fed DC Motor Drive using Interval Type-2 Fuzzy Logic Controller, Advances and Application in Mathematical Sciences, 21(11): 6571-6588.

El-Kholy, EE., Shokralla, SS., Morsi, AH. and El-Absawy, SA. 2004. Improved Performance of rolling-mill drives using fuzzy hybrid-PI controller, Electromotion, 11: 213 – 224.

Hameed, HQ. and Ali, FM. 2016. Design of a PC-based DC motor speed controller, Diyala Journal of Engineering Sciences, 9(2): 1–11.

Corresponding author's email address: geraldiyoke@mouau.edu.ng

Hareb, M., Ekhail, M. and Hareb, F. 2021. Separately Excited DC Motor Speed Control, Simulation Case Study, 1st International Mahreb Meeting of the Conference on Sciences and Techniques of Automatic Control and Control Engineering MI-STA, 47 – 51.

Hassan, AY., Rohieem, AG. and Salem, SMS. 2014. Direct torque control of non-salient pole AFPMSMs with SVPWM inverter, International Journal of Power Electronics and Drive Systems, 13(4): 2014–2023.

Hughes, A. 2006. Electric motors and drives: Fundamentals, Types and Applications, Elsevier Ltd, Linacre House, Jordan Hill, Oxford OX2 8DP, 134 – 164.

Kandpal, M., Rai, JN. and Aggarwal, A. 2015. Comparative study of Speed control of Separately Excited DC Motor using PI controller and Fuzzy Logic Controller, International Journal of Electronics, Electrical and Computational System, 4: 27 – 36.

Krishnan, R. 2001. Electric Motor Drive: Modeling, Analysis, and Control, Prentice Hall, Inc. Upper Saddle River, New Jersey, 114 – 117.

Namdeo, R., Sharma, CS. and Minz, RB. 2014. Analysis of Speed for Separately Excited dc Motor using all Types of Single-phase and Three-Phase Rectifiers, International Journal of Engineering Research & Technology (IJERT), 3(9): 305 – 312.

Nguyen, KK. and Nguyen, TT. 2019. The sensorless control system for controlling the speed of direct current motor, Indonesian Journal of Electrical Engineering and Computer Science, 16(3): 1171-1178.

Onah, AJ., Awah, CC. and Diyoke, GC. 2022. Speed Control of Direct Current Motors, Nigerian Research Journal of Engineering and Environmental Sciences, 7(1): 319 – 329.

Perelmuter, V. 2012. Electrotechnical Systems: Simulation with Simulink® and SimPowerSystems TM, CRC Press.

Poornima, P., Suganya, P., Kumaresan, N. and Subbiah, M. 2006. Operating modes of Single –phase Thyristor converter fed dc drives using Phase angle control scheme-A Monograph, IEEE International Conference on Industrial Technology, Mumbai, 2402 – 2407.

Rashag, HF. 2019. Improved speed response of DC motor via intelligent techniques, International Journal of Advances in Applied Sciences (IJAAS), 8(3): 204-207.

Saini, P., Rawat, N. and Dixit, A. 2020, Design and Analysis of Thyristor based DC Drive System for Speed Control of DC Motor, International Journal of Advanced Research in Engineering and Technology (IJARET), 11(5): 921-928.

Sami, SS., Obaid, ZA., Muhssin, MT. and Hussain, AN. 2021. Detailed modelling and simulation of different DC motor types for research and educational purposes, International Journal of Power Electronics and Drive Systems (IJPEDS), 12(2): 703-714.

Sharma, CS., Singh, K. and Tamrakar, R. 2016. A Thyristor Based Speed Control Techniques of Separately Excited dc Motor, International Journal of Scientific Development and Research (IJSDR), 1(11): 13 – 25.

Tiwari, S., Unni, AC., Rajanivedha R., Singh, GJ. and Ongsakul, W. 2019. Harmonic Analysis of Separately Excited DC Motor Drive, Innovations in Power and Advanced Computing Technologies (i-PACT), 1-7.

Virendra SS., Virendra, J. and Anil, KC. 2013. Different Speed Control Techniques of DC Motor: A Comparative Analysis, IJLTEMAS 2(7): 112 – 118.

Corresponding author's email address: geraldiyoke@mouau.edu.ng